JOURNAL OF OPTOELECTRONICS AND ADVANCED MATERIALS, Vol. 11, No. 8, August 2009, p. 1088 - 1093

Effect of structural changes during annealing on the electric and magnetic properties of $Fe_{81}B_{13}Si_4C_2$ amorphous alloy

A. MARIČIĆ, M. SPASOJEVIĆ, L. RIBIĆ-ZELENOVIĆ*, N. MITROVIĆ
Joint Laboratory for Advanced Materials of SASA, Section for Amorphous Alloys, Svetog Save 65, 32000 Čačak, Serbia

Structural changes in the $Fe_{81}B_{13}Si_4C_2$ amorphous alloy during annealing were established using differential scanning calorimetry and X-ray analysis. The alloy is stable up to 200°C. Structural relaxation occurs in the temperature interval 200-400°C resulting in short term structural ordering. Nanocrystals of the α-Fe phase form from very unordered clusters in the alloy matrix. The effect of these structural changes on magnetic and electric properties of this alloy was established. After relaxation the magnetic permeability is higher for about 18% due to the increase of mobility of magnetic domain walls and better domain directionality. At temperatures above 310°C the magnetic permeability first gradually and then rapidly decreases with temperature growth to zero value at the Curie temperature. With the increase in participation of the crystal phase in the alloy the Curie temperature increases from 410 to 590°C. In the temperature interval from 500 to 560°C crystallization occurs leading to a rapid decrease of electrical resistance. Therefore, at room temperature the crystallized alloy has a magnetic permeability about 55% lower than the as quenched amorphous alloy.

(Received July 10, 2009; accepted August 04, 2009)

Keywords: Amorphous, Ribbon, Magnetic permeability, Electrical resistance

1. Introduction

Technical progress and the development of new technologies are significantly accelerated by the development of new materials. Due to their specific electrical, magnetic, corrosive and other properties amorphous and nanostructured materials have been widely applied [1-4]. Amorphous materials are characterized by a structure where distant order atom arrangement is absent. These materials are thermodynamically unstable. During heating their structure changes relatively easily. First, structural relaxation occurs at lower temperatures. At higher temperatures crystallization occurs. These structural changes significantly change electrical, magnetic, corrosive, catalytic and other properties of these materials [4-19]. Many amorphous alloys after structural relaxation have significantly improved magnetic and other properties. However, their extremely good magnetic properties disappear after crystallization, so these materials cannot be practically applied after crystallization.

Iron and boron alloys are significant among amorphous alloys due to their soft ferromagnetic properties with a high saturation magnetic flux density. These alloys are applicable in a variety of devices, including transformers, magnetic tapes and recorder heads [20-22]. The electronic structure of iron and boron amorphous alloys is still not clear. It is not known whether boron is an electron donor or acceptor [22-26]. Replacement of boron with silica in the iron and boron alloy gradually increases the Curie temperature. This results in a sharp increase of relatively constant room-temperature saturation magnetization in $Fe_{80}B_{20}$ to $Fe_{82}B_{12}Si_6$.

The alloy crystallization temperature grows with the increase in silica and decrease of the iron and boron contents. It has been established that $Fe_{81}B_{17}Si_2$ and $Fe_{82}B_{12}Si_6$ alloys have the highest saturation magnetization, high stability and ease of preparation [27]. It has been shown that the soft magnetic properties of the Fe-B alloy improve with reduction of crystal grain size of the α-Fe phase from 20 to 10 nm. Crystallization kinetics of the $Fe_{83}B_{17}$ amorphous alloys was determined by growth of two-dimensional nucleuses [27]. However, crystallization of the $Fe_{81}B_{13}Si_4C_2$ alloy occurred in the amorphous mass by forming three-dimensional nucleuses of the α-Fe phase [28]. Three-dimensional nucleuses of different phases also formed during crystallization of the $Fe_{81}B_{13.5}Si_{3.5}C_2$ amorphous alloy [29, 30]. At temperatures slightly higher than 507°C crystals of α-Fe and Fe_2B_3 phases formed. If the temperature is significantly increased a metastable γ-Fe phase also formed [27, 28]. Atomic rearrangement and amorphous-to crystalline transformations during isothermal annealing have been investigated by Mössbauer spectroscopy [29]. It was shown that rearrangement in the amorphous state consists of two processes depending on the annealing temperature. The first process is attributed to enhancement of the short-

range order and the second one to the atomic rearrangement leading to crystallization. Crystallization was found to consist of at least two steps giving Fe_2B and Fe_3B as the final crystalline products.

The aim of this work was to investigate the effect of temperature increase of the $Fe_{81}B_{13}Si_4C_2$ amorphous alloy on microstructure changes and reflection of these changes on electric and magnetic properties.

2. Experimental

Ribbon-shaped samples $Fe_{81}B_{13}Si_4C_2$ amorphous alloy were obtained by using the standard procedure of rapid quenching of the melt on a rotating disc (melt spinning). The obtained ribbon was 2 cm wide and 35 μm thick.

Alloy crystallization was investigated by differential scanning calorimetry (DSC) in a nitrogen atmosphere using a Shimadzu DSC-50 analyzer. In this case, samples weighing several milligrams were heated in the DSC cell from room temperature to 650°C in a stream of nitrogen with flow rate of 20 cm^3 min^{-1} and heating rate of 10°C min^{-1}.

In order to investigate structural transformations by X-ray diffraction, samples of the $Fe_{81}B_{13}Si_4C_2$ amorphous alloy were annealed at different temperatures in a stream of nitrogen during 30 min. Then X-ray diffraction (XRD) patterns were recorded on a Philips PW-1710 automated diffractometer using $Cu_{K\alpha}$ radiation. The instrument was equipped with a diffracted beam curved graphite monochromator and Xe-filled proportional counter. For routine characterization diffraction data was collected in the range of 2θ Bragg angles (4-100°, counting time 0.1 s). Silicon powder was used as an external standard for calibration of the diffractometer. All XRD measurements were done with solid samples in the ribbon form at ambient temperature.

Investigation of the electrical properties was made using 20 mm x 2 mm x 35μm samples. Electrical resistance was measured by the four-point method within the temperature interval of 25°C to 600°C. The measurements were made in an argon atmosphere. Measurements of relative magnetic permeability were performed using a modified Maxwell method, based on the action of an inhomogeneous field on the magnetic sample. The magnetic force measurements were performed with a sensitivity of 10^{-6} N in argon atmosphere.

3. Results and discussion

Fig. 1 shows a DSC curve obtained by heating and cooling the $Fe_{81}B_{13}Si_4C_2$ amorphous alloy.

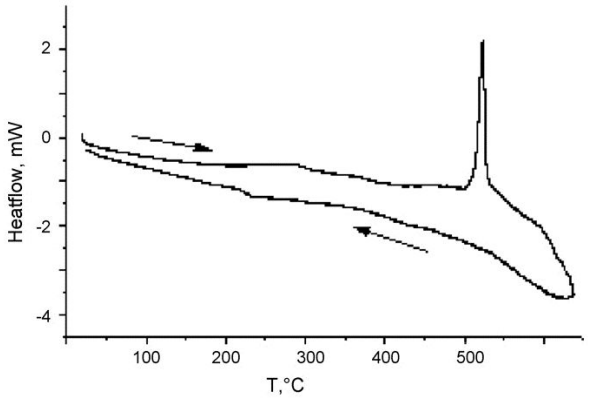

Fig.1 DSC curve of amorphous $Fe_{81}B_{13}Si_4C_2$ alloy. Heating rate 10°C min^{-1}

There are no noticeable changes in the temperature interval 25-200°C indicating that no structural changes occur in the amorphous ribbon. A weak exothermal peak in the temperature interval from 200 to 400°C is the consequence of structural relaxation. There is a sharp exothermal peak in the temperature interval from 500 to 560°C. The peak shape indicates that it is the consequence of the crystallization process. The structure of the as quenched $Fe_{81}B_{13}Si_4C_2$ alloy and nature of structural changes occurring during heating was investigated by X-ray analysis. X-ray diagrams of the as quenched alloy and alloy annealed at 50, 100 and 150°C only have a broad halo in the range 40-45°C suggesting an amorphous structure (Fig. 2).

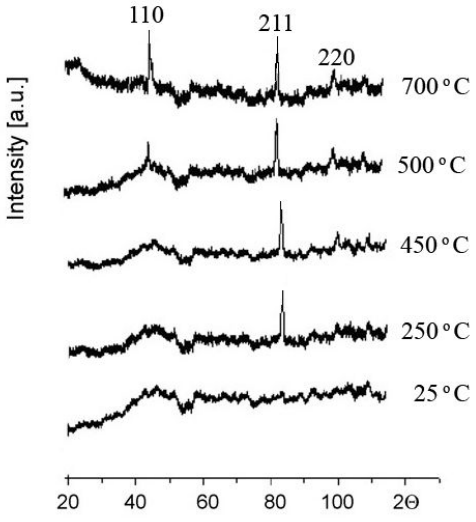

Fig.2. XRD patterns for as quenched and annealed $Fe_{81}B_{13}Si_4C_2$ alloy.

Diffractograms of the $Fe_{81}B_{13}Si_4C_2$ alloy annealed for 30 minutes at 250 °C, 300 °C, 400 °C and 450°C contain the same halo as well as the original sample, but they also contain one sharp peak at 2θ = 83,2° indicating the

presence of a structurally deformed crystal α-Fe phase as the consequence of ordering of Fe clusters already present in the starting alloy (Fig. 2). Peak intensity and half width do not significantly depend on the annealing temperature in the temperature interval of 200-450°C. This confirms that very disordered clusters are present in the as quenched alloy. During the structural relaxation process short term ordering takes place resulting in nanocrystals with a size between 5 and 20 nm.

Annealing of the $Fe_{81}B_{13}Si_4C_2$ amorphous alloy at temperatures higher than 500°C results in a new sharp peak at 2θ = 45,6° whose intensity increases as the annealing temperature grows.

The increase of intensity of that peak as well as decrease of its half width indicates the increase of alloy crystallinity. This shows that at temperatures higher than 500°C, the process of crystallization occurs. Thorough studying of diffractograms by the comparative semiqualitative analysis of the annealed alloy (JCPDS-PDF 03-065-4899) gives evidence for the presence of α-Fe crystallization in the annealed alloy. The disarranged ratio of peak intensities of diffractions lines indicates a very deformed crystal structure whose disorder disappears with the increase of temperature of annealing in accordance diffraction peak height ratios.

Curve 1 on figure 3 shows the temperature dependence of electrical resistivity of the amorphous ribbon obtained for a heating rate of 30°C min^{-1}. In the temperature interval between 25 and 500°C (A-I) the curve has an "S" shape. In the temperature interval from 25 to 200°C during heating of as quenched ribbons the heating process is stopped every 30 minutes to t_B, t_C and t_D, respectively. The change of electrical resistivity was measured simultaneously at these given temperatures (t_B, t_C and t_D). The resistivity did not change indicating that no structural changes occurred in the amorphous ribbon at these temperatures.

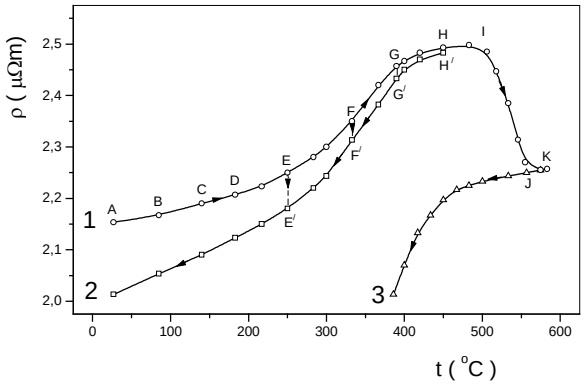

Fig. 3. Temperature dependence of electrical resistivity of amorphous $Fe_{81}B_{13}Si_4C_2$ alloy. Heating rate 30°C min^{-1}.

Low values of the temperature coefficient of electrical resistivity $\left(\frac{\partial\rho}{\partial t}\right)$ in the temperature interval from 25 to 200°C is the consequence of the increase in the number of localized electrons that move from defect states to the conduction zone as the temperature increases. In the temperature region of structural relaxation between 200 and 400°C the value of the temperature coefficient of the electrical resistivity depends on: a) short term microstructure ordering and b) the number of electrons transferring from defect states into the conduction zone. If the increase in the number of electrons transferring from defect states to the conduction zone in the temperature interval from 200 to 400°C was the same as in the interval from 25 to 200°C then the process of short term microstructure ordering would result in lower values for the temperature coefficients of resistivity in the interval from 200 to 400°C than in the temperature interval from 25 to 200°C. However, the higher value of $\left(\frac{\partial\rho}{\partial t}\right)$ in the interval from 200 to 400°C indicates that decrease in the increase rate of the number of localized electrons transferring from defect states to the conduction zone has a dominant influence on the temperature coefficient of resistivity in this interval.

However, the slope of the curve of the dependence of electrical resistivity on temperature in this temperature interval is smaller than the slope of the curve for the crystal alloy. This is the consequence of the process of short term ordering of the structure during which strongly disordered clusters transform into nanocrystals.

Short term structure ordering leads to reduction of the free volume, minimal density of chaotically distributed dislocations and mean microstrain value. These changes increase the electron mean free path and electron density of states close to the Fermi level. It is likely that the dipole moment $\vec{p}$ becomes more uniformly oriented for certain nanoparticles in certain electronic states [14].

Increase in the electron density of states $N_{(E_i)}$ and electron mean free path $\vec{l}$ and more uniformly oriented dipole moment $\vec{p}$ causes decrease in electrical conductivity in the structural relaxation temperature range according to the following relation:

$$\vec{\sigma} = \frac{N_{(E_i)} e^2 \vec{l}}{\vec{v}} \qquad (1)$$

where $\vec{v}$ is the average velocity of electrons. Since the dipole moment is given by:

$$\vec{p} = \vec{l} \cdot e \qquad (2)$$

Electrical conductivity can be described as follows:

$$\sigma = \frac{N_{(E_i)} p}{\tau} \qquad (3)$$

The presented changes resulted in a lower curve slope of the dependence of electrical resistivity on temperature for the as quenched alloy (curve 1) than the curve slope for the $Fe_{81}B_{13}Si_4C_2$ crystal alloy (curve 3) in the temperature interval from 200 to 400°C.

In this temperature interval during heating as quenched ribbons the heating process was stopped at temperatures t_E, t_F or t_G and the change of electrical resistance was measured depending on time. Short term structure ordering and formation of nanocrystals during structural relaxation caused reduction of electrical resistivity to values determined in points E', F' and G'. As quenched amorphous ribbon was also heated to 450°C and then the heating process was held for 30 minutes at this temperature. During 30 minutes of holding at t = 450°C the ribbon resistance reduced only slightly. After that the ribbon was gradually cooled with simultaneous measurement of electrical resistance. The curve obtained during cooling, marked with (2) shows the dependence of electrical resistivity on ribbon temperature in which the process of structural relaxation is completely over.

In the temperature interval from 380 to 500°C the slope of the curve of the dependence of the electrical resistivity on temperature decreases. This reduction is caused by: a) cessation of interactions between electrons in the conduction zone with magnons due to disorientation of magnetic domains and b) probable transfer of electrons from 2p – boron orbital to the 3d – iron conduction zone.

Rapid decrease of electrical resistivity with temperature increase in the interval from 500 to 560°C is the consequence of the crystallization process. After crystallization is over at temperatures above 560°C the resistance grows with temperature increase. After the maximal temperature, t_K is reached the $Fe_{81}B_{13}Si_4C_2$ alloy ribbon was gradually cooled with simultaneous measurement of electrical resistance. During cooling the electrical resistivity of the ribbon first gradually decreases from t_K to 450°C and then at temperatures lower than 420°C rapidly linearly decreases with temperature reduction. A significantly higher value of the temperature coefficient of electrical resistivity at temperatures lower than 420°C and lower value of electrical resistivity of the cooled ribbon from the values obtained for an as quenched ribbon confirm that the crystallization process occurred in the $Fe_{81}B_{13}Si_4C_2$ amorphous alloy after heating to t_K.

Structural changes in $Fe_{81}B_{13}Si_4C_2$ amorphous ribbon caused by heating lead to changes in magnetic permeability values. During the first heating of the amorphous ribbon in the temperature range from 25 do 200°C, the magnetic permeability of the alloy did not change (Fig. 4.). This indicates that structural changes in the ribbon did not take place in the above-mentioned temperature interval.

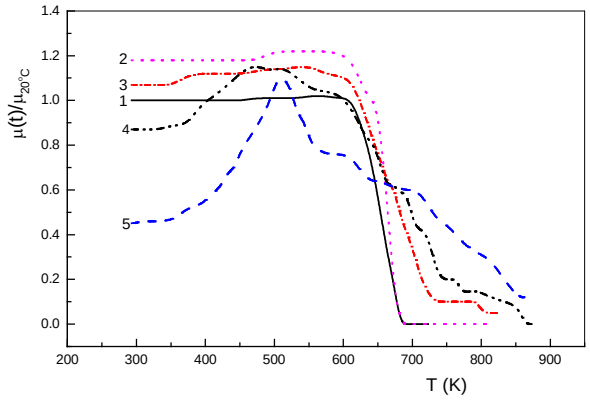

Fig. 4 Temperature dependence of the relative magnetic permeability, of $Fe_{81}B_{13}Si_4C_2$ amorphous ribbon: a) first heating up to 440°C (curve 1), second heating up to 527°C (curve 2), third heating up to 550°C (curve 3), fourth heating up to 610°C (curve 4), fifth heating up to 610°C (curve 5). Heating rate 20°C min^{-1}.

In the temperature interval from 200 to 300°C structural changes caused by temperature increase lead to increased magnetic permeability values. As we heat the alloys from 300 do 410°C, the relative magnetic permeability decreases gradually at first and then rapidly at higher temperatures, reaching zero at the Curie temperature of 410°C. Thermal energy of motion at temperatures above 410°C causes chaotically oriented magnetic domains.

After the first heating to 440°C the ribbon was cooled to 25°C and then heated again to 527°C. During the second heating the magnetic permeability did not change in the temperature interval from 25 to 200°C and its value was about 18% higher than the value of magnetic permeability of an as quenched alloy of the same composition. The increase in magnetic permeability is a consequence of the described structural changes that increase the integral of mutual interaction and consequently the energy of mutual interaction. All of these features ensure higher mobility of the magnetic domain walls and their better directionality, consequently increasing the magnetic permeability. At temperatures over 200°C the magnetic permeability first increases with temperature growth to 310°C and then with further temperature growth first gradually and then rapidly decreases to zero value at the Curie temperature. After the second heating the ribbon was cooled to 25°C and then heated again for the third time to 550°C. During the third heating the magnetic permeability did not significantly change until 310°C and had a value for about 12% lower than the value of magnetic permeability obtained for the ribbon during the second heating. This reduction of 12% is the consequence of partial crystallization of the amorphous phase in the ribbon during heating to temperatures above 500°C.

After the third heating and cooling the ribbon was heated for a fourth time to 610°C. The magnetic permeability of the ribbon cooled to 25°C after the fourth heating was for about 18% lower than the magnetic permeability of the as quenched amorphous ribbon. The

ribbon was then heated three more times to 610°C. During this heating identical values for magnetic permeability were obtained at a certain temperature. The magnetic permeability after the fourth and the following three heating cycles had a magnetic permeability value at 25°C for about 55% lower than the value obtained for an as quenched ribbon sample. This reduction of 55% is the consequence of total crystallization of the amorphous phase.

The curves given in figure 4 show that the Curie temperature value increases with growth of the participation of the crystal phase. This increase is due to formation of a crystal phase of the interstitial solid solution of boron and carbon with iron.

A detailed analysis of structural changes in $Fe_{81}B_{13}Si_4C_2$ amorphous alloy ribbons occurring during heating and reflection of these changes on electrical resistance and magnetic permeability values showed that a defined correlation exists between the alloy microstructure and its electrical and magnetic properties.

4. Conclusions

Differential scanning calorimetry and X-ray analysis were used to establish changes in the $Fe_{81}B_{13}Si_4C_2$ amorphous alloy shows that the alloy is stable in the temperature interval from 25 to 200°C so its magnetic properties do not change. The temperature coefficient of electrical resistance has a low value as with temperature increase in this interval the number of localized electrons moving from defect points to the conduction zone increases significantly. Structural relaxation occurs in the interval between 200 and 400°C where short term ordering of the structure occurred and nanocrystals of the α-Fe phase form from strongly disordered clusters in the as quenched alloy matrix. The temperature coefficient of electrical resistance in the relaxation region grows as short term ordering is not enough to compensate for the reduction of the number of localized electrons moving from defect points to the conduction zone. Structural changes during relaxation lead to increased magnetic permeability as they enable higher mobility of magnetic domain walls and better directionality of magnetic moments.

At temperatures higher than 310°C with temperature growth the magnetic permeability first gradually and then rapidly reaches zero value at the Curie temperature. The Curie temperature increases from 410 to 610°C with the increase of the crystal phase in the alloy.

In the temperature region from 380 to 500°C the value of the temperature coefficient of electrical resistance decrease due to reduced interactions between magnons and electrons from the conduction zone and probably due to transfer of localized 2p-electrons of boron atoms into the conduction zone.

The rapid decrease of electrical resistance in the temperature region from 500 to 560°C is due to the crystallization process. The crystal alloy at room temperature has a magnetic permeability that is about 55% lower than the value measured for the as quenched amorphous alloy.

The presented results show that a defined correlation exists between the $Fe_{81}B_{13}Si_4C_2$ alloy microstructure and its electrical and magnetic properties.

Acknowledgements

The Ministry for Science and Technology of the Republic of Serbia supported this investigation, under Project 142 011 G.

References

[1] J. D. Bernal, Nature, **185**, 68 (1960).
[2] H. Sterb, H. Warlimont. Rapidly Quenched Metals, Elsevier, Amsterdam, 1985.
[3] L. A. Jakobson, J. Mc. Kittrik, Rapid Solidification Processing, Elsevier, 1994.
[4] Yu. A .Kunitsky, V. I. Lisov, T. L. Tsaregadskaya, O. V. Turkov, Sci. Sintering, **35**, 391 (2003).
[5] M. V. Sušić, A. M. Maričić, Mat. Chem. Physics. **19**, 517 (1998).
[6] A Maričić, M. Spasojević, L. Rafailović, V. Milovanović, L. Ribić-Zelenović, Mater. Sci. Forum **453**, 411 (2004).
[7] N. Mitrović, S. Roth. J. Eckert, C. Mickel, J. Phys. D: Appl. Phys. **35**, 2247 (2002).
[8] L. Ribić-Zelenović, L. Rafailović, M. Spasojević, A. Maričić, Sci. Sintering **38**, 145 (2006).
[9] S. Randjić, A. Maričić, L. Rafailović, M. Spasojević, M. M. Ristić, Sci. Sintering **38**, 139 (2006).
[10] L Ribić-Zelenovć, R. Simeunović, A. Maričić, M. Spasojević, Mater. Sci. Forum **555**, 539 (2007).
[11] J. S. Song, H. B. Im. M. S. Yun, J. Appl. Phys. **69**(8) 5014 (1991).
[12] L. Ribić-Zelenović, L. Rafailović, A. Maričić, M. Spasojević, J. Optoelectr. Adv. Mater. **9,** 2681 (2007).
[13] V. E. Egoruskin, N. V. Melnikova, Metalofizika, T. **10**(1), 81 (1988).
[14] L. Ribić-Zelenović, L. Rafailović, M. Spasojević, A. Maričić, Physica B 403, 2348 (2008).
[15] A. P. Spak, V. L. Karbovskij, A. N. Jaresko, Metalofizika i noveisie tehnologii, **16**(3), 32 (1994).
[16] L. Ribić-Zelenović, L. Rafailović, A. Maričić, M. Spasojević, J. Optoelectr. Adv. Mater. **10,** 1384 (2008).
[17] A.P.Spak, V.L. Karbovskij, Bliznij poredak i osobennosti elektronnoj strukturi v amorfnih metalliceskih splavah na osnove 3d metallov, KNMF, (1994) 44.
[18] M. Spasojević, A. Maričić, L. Rafailović, Sci. Sintering **36**, 105 (2004).
[19] L.Ribić-Zelenović, M.Spasojević, A. Maričić, Mater. Chem. Physics, **115**, 347 (2009).
[20] R. A. Cowley, D. Mick, Paul, W. G. Stirling, S. N. Cowlam, Physica **120B**, 373 (1983).

[21] N. Cowlam, J. Non-Cryst.Solids, **205-207,** 567 (1996).
[22] S. D. Kaloshkin, L. A. Tomilin, Thermochim. Acta, **280-281**, 303 (1996).
[23] O.Yu. Kontsevoi, V.A. Gubanov, Phys. Rev.B, **51**, 15125 (1995).
[24] R.F. Sabiryanov, S.K.Bose, O.N. Mryasov, Phys. Rev. B, **51,** 8958 (1995).
[25] T. Fujiwara. J.Phys. F: Metal Phys, **661-675**, 12 (1982).
[26] J. Hafher, M. Tezge, C R. Becker, Phys. Rev. B, **285-298**, 49 (1994).
[27] F. E. Luborsky, J. J. Becker, J. L. Walter, H. H. Liebermann, IEEE Trans.Magn. **15**, 1146 (1979).
[28] D.R. dos Santos, D.S. dos Santos, J. Non-Cryst. Solids **304**, 56 (2002).
[29] N. Segusa, A. H. Morrish, Phys. Rev. B. **26**, 305 (1982).
[30] D. M. Minić, A. Maričić, B.Adnađević, J. Alloys Compd. **473**, 363 (2009).

*Corresponding author: lenka@tfc.kg.ac.rs